University of Baghdad
College of Engineering
JOURNAL OF ENGINEERING

Journal of Engineering

journal homepage: www.joe.uobaghdad.edu.iq
Number 10 Volume 24 October 2018

Mechanical and Energy Engineering

Experimental Study of Hybrid Solar Air Conditioning System in Iraq

Ahmed Abd Mohammed*
Assistant Professor
Mechanical Engineering Department
University of Technology
email: 20187@uotechnology.edu.iq

Raed Ayad Abduljabbar
Assistant Lecturer
Mechanical Engineering Department
University of Technology
email: me.21148@uotechnology.edu.iq

ABSTRACT

In this paper, an experimental study of the thermal performance for hybrid solar air conditioning system was carried out, to investigate system suitability for the hot climate in Iraq. The system consists of vapor compression unit combined with evacuated tube solar collector and liquid storage tank. A three-way valve was installed after the compressor to control the direction flow of the refrigerant, either to the storage tank or directly to the condenser. The performance parameters were collected by data logger to display and record in the computer by using LabVIEW software. The results show that the average coefficient of performance of hybrid solar air conditioning system (R=1) was about 2.42 to 2.77 and the average power consumption was about 1.1 to 1.12 kW when the ambient temperature was about 34.2 to 39.7 ˚C, while the average coefficient of performance of conventional system (R=0) was about 3.23 and the average power consumption was about 1 kW when the ambient temperature was about 30.8 to 34.3 ˚C. It can be concluded that the use of the hybrid solar system in Iraq with its current form could not be saved electricity.

Key Words: hybrid system, evacuated tubes collector, vapor compression cycle.

دراسة تجريبية لنظام تكييف الهواء الشمسي الهجين في العراق

احمد عبد محمد
استاذ مساعد
قسم الهندسة الميكانيكية
الجامعة التكنولوجية

رائد اياد عبد الجبار
مدرس مساعد
قسم الهندسة الميكانيكية
الجامعة التكنولوجية

الخلاصة

تم إجراء دراسة تجريبية لاختبار الأداء الحراري لنظام تكييف الهواء الشمسي الهجين ورؤية مدى ملائمته للاجواء الحارة في العراق. يتكون النظام من دورة بخار انضغاطية مدمجة مع مجمع شمسي من نوع الانابيب المفرغة بالاضافة الى خزان الماء الحار. تم تركيب صمام ثلاثي الاتجاه بعد الضاغط مباشرة للتحكم في اتجاه جريان مائع التثليج ، حيث يكون اتجاه جريان مائع التثليج اما باتجاه خزان الماء الحار (كما في النظام الهجين) أوباتجاه المكثف مباشرة (كما في النظام التقليدي). تم جمع معاملات الأداء بواسطة مسجل البيانات، وتم عرضها وتسجيلها في جهاز الحاسوب باستخدام برنامجLabView. أظهرت النتائج أن متوسط معامل أداء النظام الهجين (R=1) كان يتراوح ما بين 2.42 الى 2.77 ، وكان متوسط استهلاك الطاقة الكهربائية ما بين 1.1 إلى 1.12 كيلوواط عندما كانت درجة حرارة الهواء الخارجي ما بين 34.2 إلى 39.7 درجة مئوية، في حين أن متوسط معامل أداء النظام التقليدي(R=0)كان حوالي 3.23 ومتوسط استهلاك الطاقة الكهربائية حوالي 1 كيلوواط عندما كانت

*Corresponding author
Peer review under the responsibility of University of Baghdad.
https://doi.org/10.31026/j.eng.2018.10.03

Article accepted:6/12/2017

درجة حرارة الهواء الخارجي ما بين 30.8 إلى 34.3 درجة مئوية، لذلك فان استخدام النظام الهجين في العراق بشكله الحالي قد لا يوفر طاقة كهربائية.

كلمات البحث الرئيسية:النظام الهجين، مجمع شمسي ذو انابيب مفرغة، دورة البخار الانضغاطية.

1. INTRODUCTION

A considerable increase in the global electricity demand and depletion of fossil fuel resources have increased the need for the development of eco-friendly and energy-efficient technologies, **Desideri, et al., 2009**. The consumption of electricity in Iraq is higher than production, and the air conditioning demand has increased rapidly in the recent years, which represents globally about 55% of total building energy consumption due to the demand of higher comfort conditions inside buildings, **Al-Abidi, et al., 2012**. Hence, a solar hybrid air conditioning system seems to be the solution to electricity leak. Compared with conventional energy, solar energy has many advantages, such as inexhaustibility, cleanness, and cheapness. **Ha and Vakiloroaya, 2012,** enhanced the performance of direct expansion air conditioner when combined with a vacuum solar collector that is installed after the compressor. A by-pass line was proposed together with a three-way proportional control valve so the refrigerant flow rate is controlled and then the optimum refrigerant temperature entering the condenser is estimated. **Vakiloroayaet, al., 2012** analyzed the performance of a new solar-assisted air conditioner to achieve energy saving. A flat collector storage system was equipped with the evaporator to raise the superheat temperature entering the compressor. They showed that the compressor can be turned off longer and thus reduce the power consumption. The system was promising for saving average monthly electricity by up to 40%. **Abd, et al., 2013,** studied experimentally the thermal performance of hybrid solar assisted air conditioning system with and without water in the storage tank. They noticed that the refrigerant temperature and pressure leaving the solar collector were decreased, and the average thermal efficiency was fairly acceptable. **Vakiloroaya, et al., 2013,** developed a hybrid solar air conditioning system by proposing a new discharge bypass line together with an inline solenoid valve to increase the subcooling of the refrigerant at partial loads, the solenoid valve installed after the compressor was to regulate the mass flow rate of the refrigerant. This development is promising between 25 and 43% of monthly electricity can be saved on average .**Abid and Jassim, 2015,** investigated an experimental study of the thermal performance of air conditioning system combined with a solar collector. The prototype consisted of three different process fluid loops: air conditioning loop, collector loop, and cooling tower loop. The bypass installed after compressor was to control the flow rate of the refrigerant. Results showed that the compressor power consumption was decreased from 1.2 kW at solar radiation 572 W/m^2 to 0.9 kW at solar radiation 725 W/m^2, this led to increase in COP from 2.49 to 2.72. The average energy saving of power consumption is between 23% and 32%. **Kumar et al., 2016,** introduced their study of performance analysis of solar hybrid air conditioning system which consists of R410a vapor compression refrigeration cycle cascaded with solar driven. The average coefficient of performance was about 2.71. The objective of present work is to study the performance of the hybrid solar air conditioner system with the aid of bypass line with the three-way actuator valve to overcome insufficient solar radiation in a day in Iraq (hot zone).

2. EXPERIMENTAL WORK

The rig consists of seven main components which are: rotary compressor, air-cooled condenser, an expansion device (capillary tube), direct expansion evaporator, vacuum solar collector, storage tank, and three-way control valve and test room. **Fig. 1**and **Fig. 2** show a schematic block diagram and a photo of the system, respectively.

2.1 Compressor

Hermetic rotary compressor model (RS208VCDC) Mitsubishi electric with 3.5 kW cooling capacity and using R22 as a working fluid.

2.2 Condenser (Outdoor Unit)

Finned and tube condenser with two rows and 20 tubes per row, the length of each row is 75 cm, and the outer tube diameter is 9.57 mm, the output power of condenser fan is 20 W.

2.3 Evaporator (Indoor Unit)

Direct expansion evaporator with one row and 26 tubes per row, the length of the row is 65 cm and outer tube diameter is 7.6 mm.

2.4 Evacuated Tubes Collector

The evacuated tubes solar collector consists of 10 tubes, each tube has 45 cm length and consists of two glass tubes, and the outer diameter of the inner tube is 3.7 cm. The outer diameter of the outer tube is 4.7 cm. The space between inner and outer tubes is evacuated, the inner and outer tubes are domed at one end. The inner tube is made up of Borosilicate type material which has excellent characteristics of light transparency (> 92% and 2mm thick). The surface of the inner tube is coated with the selective surface to be an absorber surface. The bottom side of evacuated tubes is made up of the aluminum plate, and the upper side of evacuated tubes passes through the storage tank.

2.5 Storage Tank with Heat Exchanger

A horizontal cylindrical tank with 20 cm outer diameter and 80 cm length, the tank is insulated with 2 cm thickness of foam to prevent the heat loss due to convection, the capacity of the tank and collector is 18 liter. A filling water pipe with 12.5 mm diameter passes through the tank from the upper side to fill the collector and the tank with distilled water. A spiral copper coil with 9.57 mm outer diameter is immersed inside the tank where the refrigerant flows inside it. The solar collector absorbs the solar energy and heats the water in the evacuated tubes, the hot water flows towards the storage tank naturally due to the difference in densities. So the water in the storage tank is heated continuously by the solar collector. The storage tank with a coiled tube is used as a heat exchanger (source) to increase refrigerant temperature.

2.6 Three-Way Valve

A three-way control valve model (LPA14-403B9CPC3-10-64) is installed after the compressor to regulate the flow direction of the refrigerant either to the condenser or to the storage tank.

2.7 Test Room

A sandwich panel room was constructed to represent the conditioning space. The dimensions of the room are 2×2×2 m. The evaporator was installed inside the room, while the

compressor, condenser, capillary tube, three-way control valve, vacuum solar collector, and storage tank were installed outside the room. The aim of constructing this room is to control the indoor conditions, also this room protects the electronic devices (like data acquisition and computer) from outdoor conditions and provides the appropriate operating conditions. Two electrical heaters with 1000 W each was installed inside the room to simulate thermal load to prevent very low temperature and then stop the system.

3. MEASURING DEVICES AND DATA LOGGING

The parameters data of the present work were displayed and recorded automatically as listed in **Table 1**.

Negative thermal coefficient thermistor (NTC) is used to measure the temperature, the operating temperature range of NTC is -40 to 125 ˚C. **Fig. 3** and **Fig. 4** show the NTC and its fixing on the tube surface, respectively. A pressure transducer (Danfoss) is used to measure refrigerant pressure, power supply 24 V DC, error 1 % and 1/3 inch male thread. The operating pressure range of pressure transducer at the suction line (P1) is 0 to 10bar and its output signal is 0 to 5 V, while the operating pressure range of (P2, P6, P8) is 0 to 50 bar and the output signal is 0 to 10 V. The gas flow meter is installed at the suction line to measure refrigerant flow rate. The flow meter model is CX-LWGQ-15AMC4, DN 15 male thread, the power supply is 24 V DC, the analog output signal is4 to 20 mA DC in addition to pulse screen display, the operating flow range is 1.5 to 5 m^3/hr, the error is 2.5 %. Solar power meter (TES 1333R) is used to measure the total solar radiation (beam, diffuse and reflected) in W/m^2, it is oriented to the south and inclined by 20˚ with the horizon (same as a solar collector). Potential transformer (PT) and current transformer (CT) were used to measure the voltage and current of the system respectively, national instrument (NI) data acquisition, 32 port, and input power 11-30 V DC, 50 W is used to record and display data on the computer.

4. TEST PROCEDURES

All tests were carried out in Baghdad (latitude angleϕ is 33.3˚) on September 2016. The solar collector was oriented to the south and tilted (β) by 20˚ with the horizon to get optimum solar radiation, **Duffie, and Beckman, 2013**. A metal frame was manufactured to achieve this purpose. The system was charged with R22.

For each test, the following procedures were followed:

- The solar collector and the storage tank were filled with distilled water.
- The evacuated tubes were cleaned.
- The system was turned on.
- The computer and control program was turned on.
- Set the opening valve ratio, either fully opened to the solar collector and its storage tank (R=1) or fully opened to the condenser with bypass line as a conventional system (R=0).
- Solar radiation intensity was measured each half hour.
- Record all the parameter data (listed in Table 1) in the computer by data logger every two minutes.

5. PARAMETERS CALCULATIONS

The power consumption of the system can be calculated by the following equation:

$$P_{cons.} = V \times I \quad (1)$$

And the cooling capacity of the evaporator is expressed as:

$$Q_e = \dot{m}_r \times (h9 - h8) \quad (2)$$

While the coefficient of performance of the system is calculated by:

$$COP = \frac{Q_e}{P_{cons.}} \quad (3)$$

6. RESULTS AND DISCUSSIONS

Many experimental tests were carried out on the system to study its thermal performance and compare it with the conventional system, just three tests are discussed in this paper as samples to other tests, and each test is studied within four characteristic parameters as following:

6.1 Refrigerant Temperature

Fig. 4 represents the p-h diagram for test 1 at 12:30 PM, where the refrigerant temperature was shown along the cycle as well as other parameters.

Fig.s 5a, 5b, and **5c** represent the refrigerant temperature at five positions with time, where the x-axis represents time in minutes and the y-axes represent temperature in degree centigrade. From these figures, it's clear the transition period was taken about 16 minutes until the system reaches the stability. The average refrigerant temperature inlet the compressor (T1) was 10.8 ˚C at first 170 minutes, then it dropped to 4.1˚C with low room temperature due to insufficient thermal load inside the room, **Fig. 5a**. While the average values of T1 were 9.8 and 7.4 ˚C in **Fig. 5b** and**5c**, respectively.

The refrigerant outlet temperature from the compressor (T2) has approximately the same behavior in each test but with some difference in values, where T2 increased with time until the system reached the steady state (after 16 minutes), then it slightly fluctuated with time. The values of T2 is considered relatively high due to the low isentropic efficiency of the compressor and high ambient temperature. The average value of T2 is about 100.6 ˚C in **Fig. 5a**, and 97.7 ˚C in **Fig. 5b**. While average T2 is89.9 ˚C in **Fig. 5c**, which is less than the other due to low ambient temperature.

It is important to observe that the refrigerant temperature inlet the condenser (T6) is still below T2 which may be caused by the reverse action in the storage tank (decrease the refrigerant temperature instead of increase it due to losing a part of its sensible heat to the water) as shown in **Fig. 5a** and **Fig. 5b**. T6 depends on two parameters, T2, and three-way valve ratio R (0 or 1) and it determined the degree of subcooling in the condenser, therefore it can be used as a control variable signal to optimize the three-way valve opening.

The refrigerant temperature inlet and outlet the evaporator (T7 and T8) have the same behavior in all figures and they slightly fluctuated with time.

6.2 Air and Water Temperature

Fig.s 6a, 6b and **6c** represent air and water temperature with time, where the x-axis represents time recorded and the y-axis represents the inlet and outlet air temperature of the condenser and evaporator and water temperature in the storage tank.

The water temperature in the storage tank (T_w) increased with time due to increases in solar radiation intensity at approximately first 160 minutes, then it approximately became constant with time due to heat balancing between the solar radiation and hot gas refrigerant (outlet from the compressor). T_w ranged from 56.1 to 92.4 ˚C in **Fig. 6a** and from 65.6 to 92.5 ˚C in **Fig. 6b**.

The air temperature inlet to the condenser ($T_{\text{air cond. in.}}$) is very close to ambient temperature ($T_{\text{amb.}}$) and they can be considered identical, while the air temperature outlet the condenser ($T_{\text{air cond. out.}}$) depend on air temperature inlet the condenser and T6.

The air temperature inlet the evaporator ($T_{\text{air evap. in.}}$) is very close to room temperature (T_{room}) and it can be considered identical. The average air temperature difference across the evaporator ranged from 12.5 to 15˚C and the fluctuating inlet and outlet temperature refers to internal load (heater) inside the test room as shown in **Fig. 6a**.

6.3 Refrigerant Pressure and Flow Rate

The refrigerant pressure and volumetric flow rate with time are represented in **Fig. 7a**, **7b,** and **7c.** The pressure P1, P2, P6 and P8 increased and decreased with time according to the ambient temperature. The average values of P1, P2, P6, and P8 are (4.8, 20.1, 19.5 and 6.1 bar) respectively. It is noticed that P6 is slightly below P2 due to the pressure loss across the storage tank, also there is a pressure drop across the evaporator as shown in **Fig. 4.**

The flow rate ($\dot{V}_r$) slightly oscillated with time for first 174 minutes, then increased due to the increase in the temperature difference of air and refrigerant inlet the evaporator as shown in **Fig. 7a**. The average flow rate is 3.43 m^3/hr, and it slightly fluctuated with time to3.5 m^3/hr as shown in **Fig. 7b**. The refrigerant flow rate plays an important role in the evaporator cooling capacity. The cooling capacity (Q_e) ranged from 2364 to 3290 W (0.67 to 0.93 TR) as shown in **Fig. 8a** later.

6.4 Power Consumption, Cooling Capacity, Solar Radiation Intensity and Coefficient of Performance

The representation of power consumption, evaporator cooling capacity, solar radiation intensity and coefficient of performance are depicted in **Fig. 8a**, **8b,** and **8c**.

The power consumption of the system is varied with time according to the variation in the thermal load.

The solar radiation intensity increased with time until solar noon, the maximum value is about 600 W at noon.

The average value of COP is about 3.23 in **Fig. 8c**, while its average values are 2.42 and 2.77 as shown in **Fig. 8b** and **8c,** respectively. It is clear that COP in **Fig. 8c** is higher than COP in **Fig. 8a** and **8b** because of the higher cooling capacity and lower power consumption.

7. CONCLUSIONS

1. Average COP of hybrid solar air conditioning system is less than the average COP of the conventional system by 14 %.
2. The average power consumption of hybrid solar air conditioning system is higher than the average power consumption of the conventional system by 10 %.
3. In hybrid solar air conditioning system, the refrigerant temperature inlet to the condenser is still less than the refrigerant temperature outlet from the compressor, that is mean the utilization of solar system is useless in this study.

REFERENCES

- Abd, S. S., Owaid, A. I., Mutlak, F. A., and Sarhan, A. R., 2013, *Construction and Performance Study of ASolar-Powered Hybrid Cooling System in Iraq*, Iraqi Journal of Physics, Vol. 11, No. 21, PP. 91-101.

- Abid, M. A., and Jassim, N. A., 2015, *Experimental Evaluation of Thermal Performance of Solar Assisted Air Conditioning System under Iraq Climate*, Journal of Energy Technologies and Policy, Vol. 5, No. 12, PP. 1-13.

- Al-Abidi, A. A., Mat, S. B., Sopian, K., Sulaiman, M.Y., Lim, C.H., Abdulrahman, T. h., 2012, *Review of Thermal Energy Storage for Air Conditioning Systems,* Renewable, and Sustainable Energy Reviews, Vol. 16, PP. 5802-5819.

- Desideri, U., Proietti, S., and Sdringola, P., 2009, *Solar-Powered Cooling Systems: Technical and Economic Analysis on Industrial Refrigeration and Air-Conditioning Applications,* Applied Energy, Vol. 86, PP. 1376-1386.

- Duffie, J. A., and Beckman, W. A., 2013, *Solar Engineering of Thermal Processes*.John Wiley & Sons, Inc., Hoboken, New Jersey.

- Ha, Q. P., and Vakiloroaya, V., 2012, *A Novel Solar-Assisted Air-Conditioner System for Energy Savings with Performance Enhancement*, Procedia Engineering Vol. 49, PP. 116-123.

- Kumar, S., Buddhi, D., and Singh, H. K., 2016, *Performance Analysis of Solar Hybrid Air-Conditioning System with Different Operating Conditions*, Imperial Journal of Interdisciplinary Research (IJIR), Vol. 2, No. 10, PP. 1951-1956.

- Vakiloroaya, V., Ha, Q. P., and Samali, B., 2012, *Experimental Study of A New Solar-Assisted Air-Conditioner for Performance Prediction and Energy Saving*, Australian Congress on Applied Mechanics (ACAM), Vol. 7, No. 16, PP. 768-777.

- Vakiloroaya, V., Ismail, R., and Ha, Q. P., 2013, *Development of A New Energy-Efficient Hybrid Solar-Assisted Air Conditioning System*, International Symposium on Automation and Robotics in Construction and Mining (ISARC), Vol. 30, PP. 1424-1435.

NOMENCLATURE

COP = coefficient of performance, dimensionless.

G_T = solar radiation incident on the collector plane, W.

h8 = refrigerant enthalpy inlet the evaporator, kJ/kg.

h9 = refrigerant enthalpy outlet the evaporator,kJ/kg.

I = current passes through the system, A.

$\dot{m}_r$ = refrigerant mass flow rate, kg/s.

P1 = refrigerant pressure inlet to compressor, bar.

P2 = refrigerant pressure outlet from compressor, bar.

P6 = refrigerant pressure inlet to condenser, bar.

P8 = refrigerant pressure inlet to evaporator, bar.

$P_{cons.}$ = power consumption by the system, W.

Q_e = cooling capacity of the evaporator, W.

R = ratio of the opening valve to the storage tank to the opening valve to condenser directly, dimensionless.

T1 = refrigerant temperature inlet to the compressor, ˚C.

T2 = refrigerant temperature outlet from the compressor, ˚C.

T3 = refrigerant temperature inlet to the storage tank, ˚C.

T4 = refrigerant temperature outlet from the storage tank, ˚C.

T5 = refrigerant temperature in the bypass line, ˚C.

T6 = refrigerant temperature inlet to the condenser, ˚C.

T7 = refrigerant temperature outlet from condenser, ˚C.

T8 = refrigerant temperature inlet to the evaporator, ˚C.

T9 = refrigerant temperature outlet from the evaporator, ˚C.

$T_{air\ evap.\ in.}$ = air temperature inlet to the evaporator, ˚C.

$T_{air\ evap.\ out.}$ = air temperature outlet from the evaporator, ˚C.

$T_{air\ cond.\ in.}$ = air temperature inlet to condenser, ˚C.

$T_{air\ cond.\ out.}$ = air temperature outlet from condenser, ˚C.

$T_{amb.}$ = ambient dry bulb temperature, ˚C.

T_{room} = room temperature, ˚C.

T_w = water temperature in the thestorage tank, ˚C.

V = voltage passes through the system, v.

$\dot{V}_r$= volumetric flow rate of refrigerant in the suction line, m^3/hr.

β = collector slope angle, degree.

ϕ = latitude angle, degree.

Table 1. Measuring data.

No.	Parameters	Notation
1	Refrigerant temperature before and after each component.	T1- T9
2	Refrigerant pressure before and after the compressor.	P1, P2
3	Refrigerant pressure before condenser and evaporator.	P6, P8
4	Refrigerant flow rate.	$\dot{V}_r$
5	Water temperature of the storage tank.	T_w
6	Inlet and outlet air temperature of the condenser and evaporator.	$T_{\text{air evap. in.}}$, $T_{\text{air evap. out.}}$, $T_{\text{air cond. in.}}$, $T_{\text{air cond. out.}}$
7	Ambient and room temperature.	$T_{\text{amb.}}$, T_{room}
8	Voltage and current of the system.	V, I

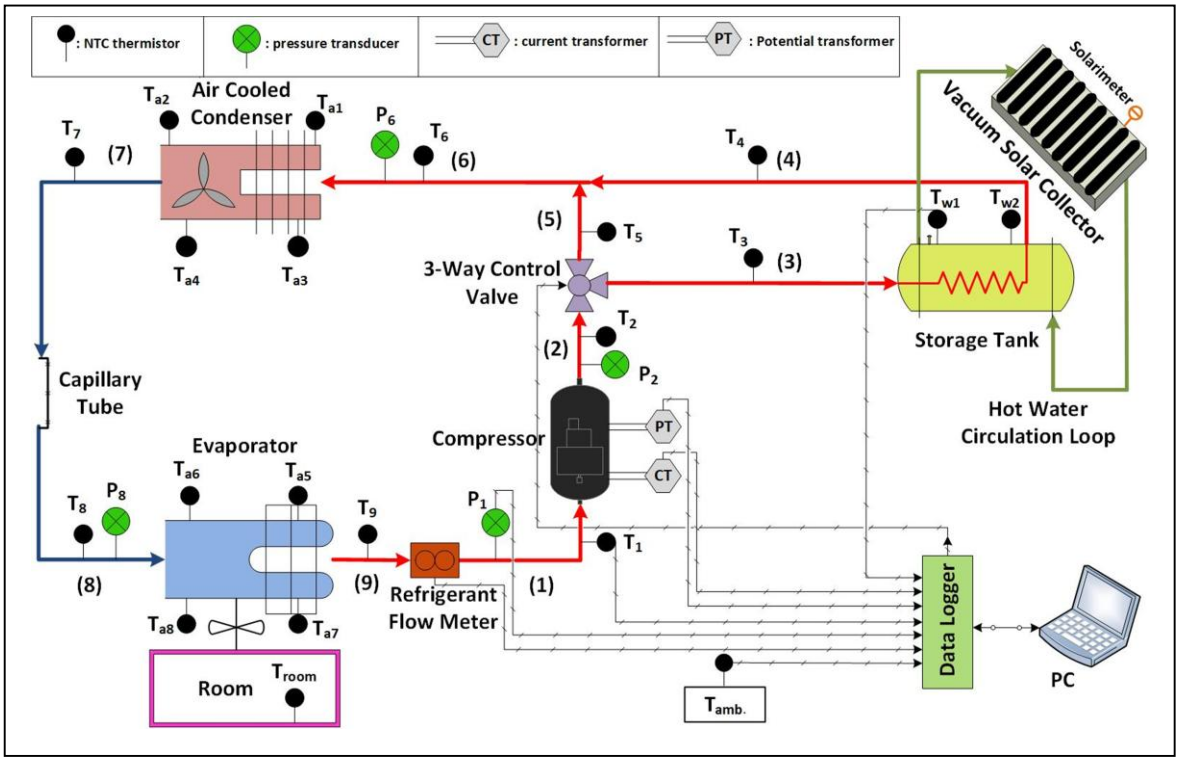

Figure 1. Schematic block diagram of the hybrid solar air conditioning system and its control system.

Figure 2. Photo of the test rig.

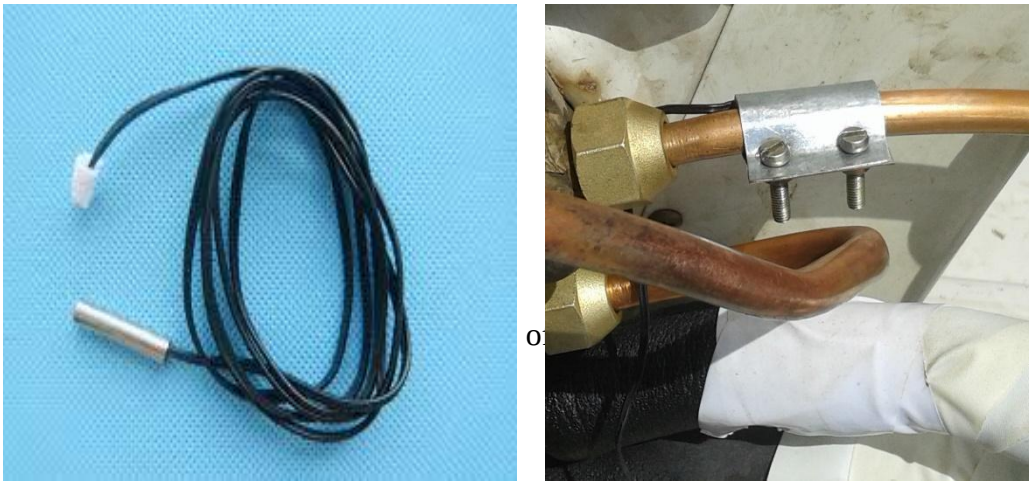

Figure 3. Photo of NTC thermistor and fixing it on tube surface.

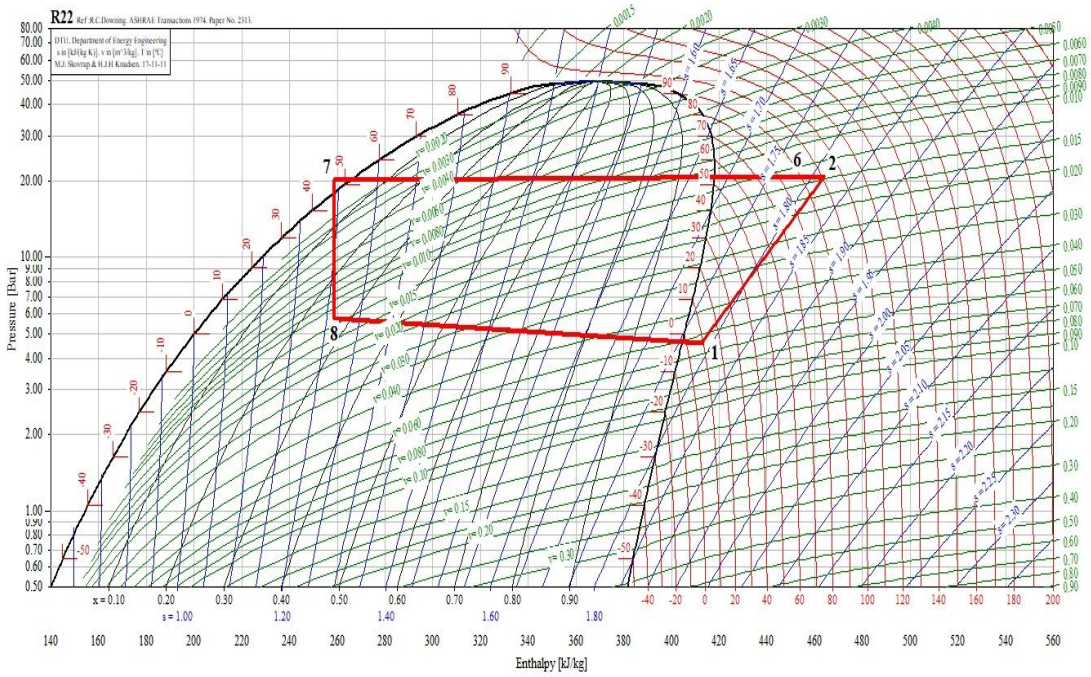

Figure 4. P-h diagram for test (1) at 12:30 PM.

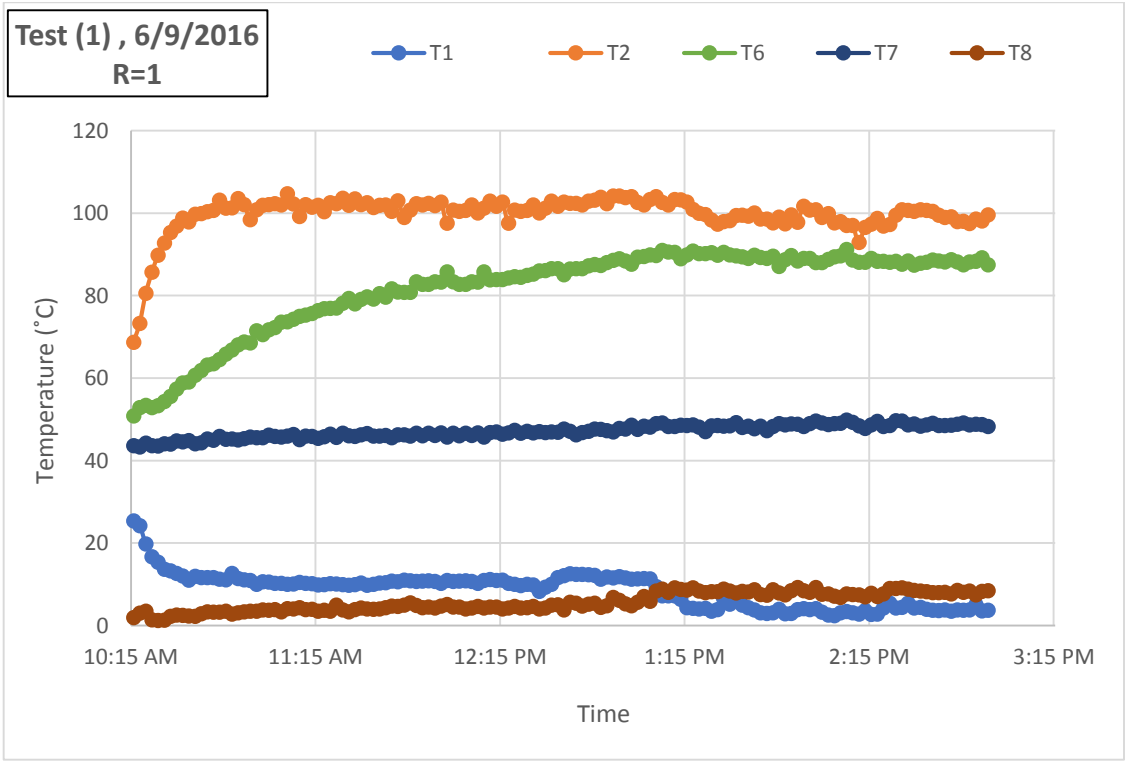

Figure 5a. Refrigerant temperature with time for test (1).

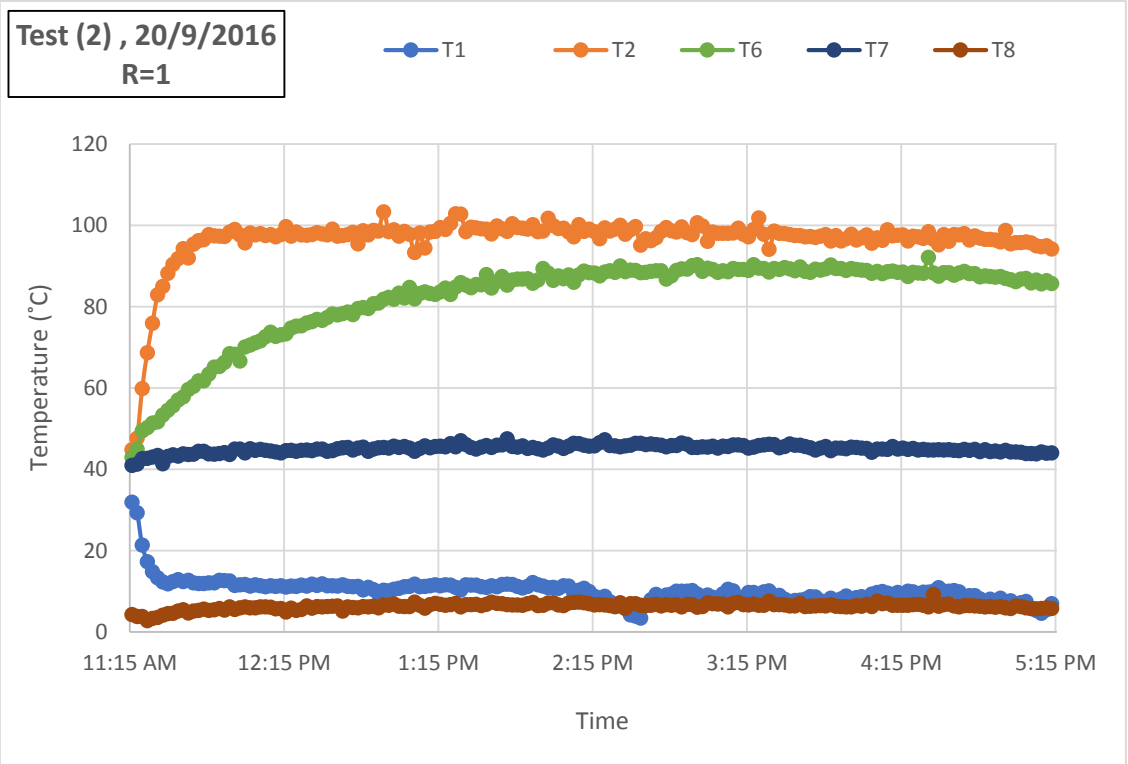

Figure 5b. Refrigerant temperature with time for test (2).

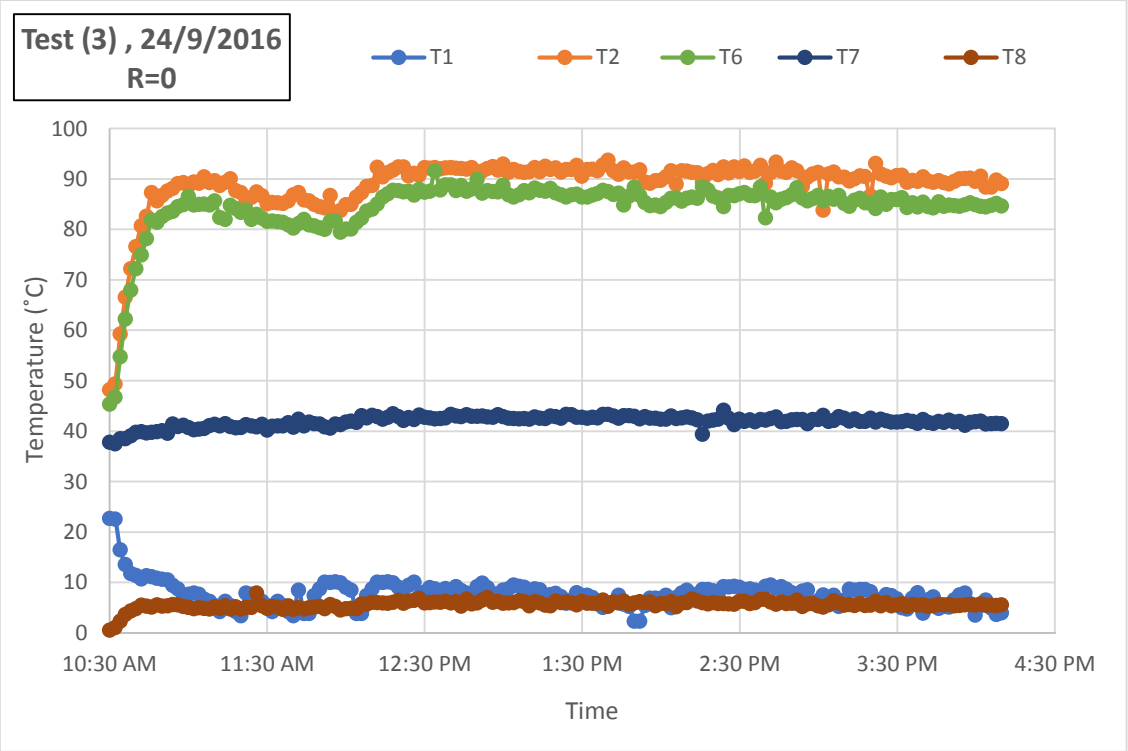

Figure 5c. Refrigerant temperature with time for test (3).

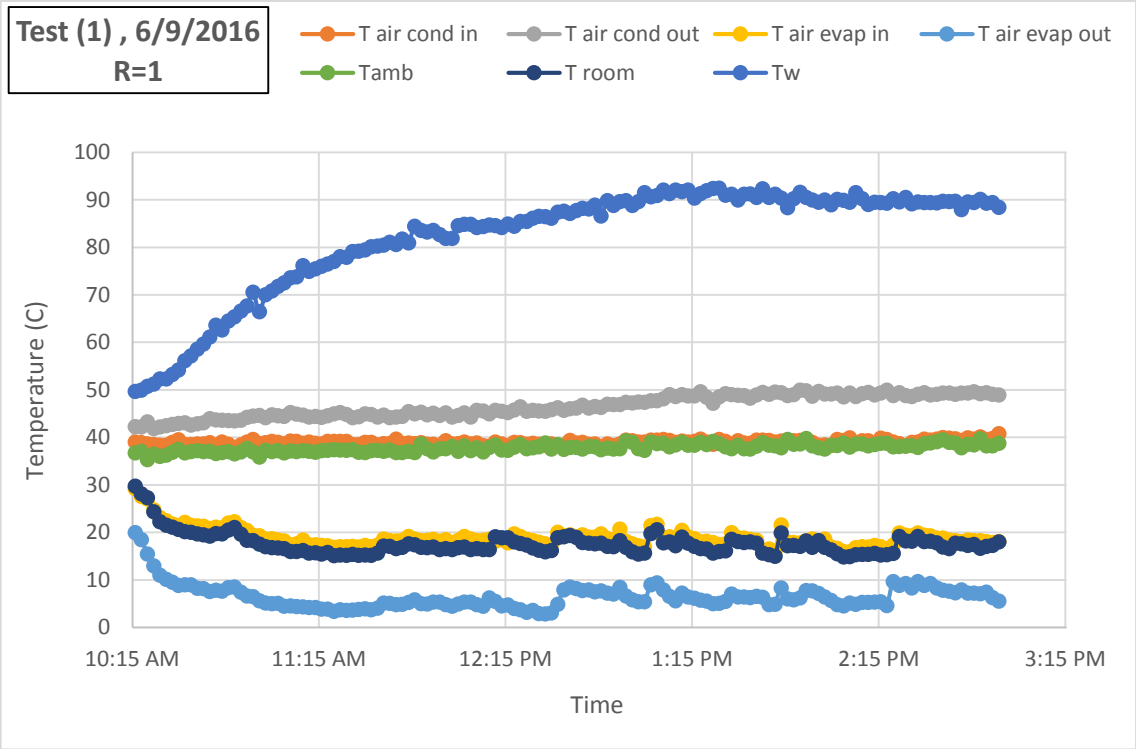

Figure 6a. Air and water temperature with time for test (1).

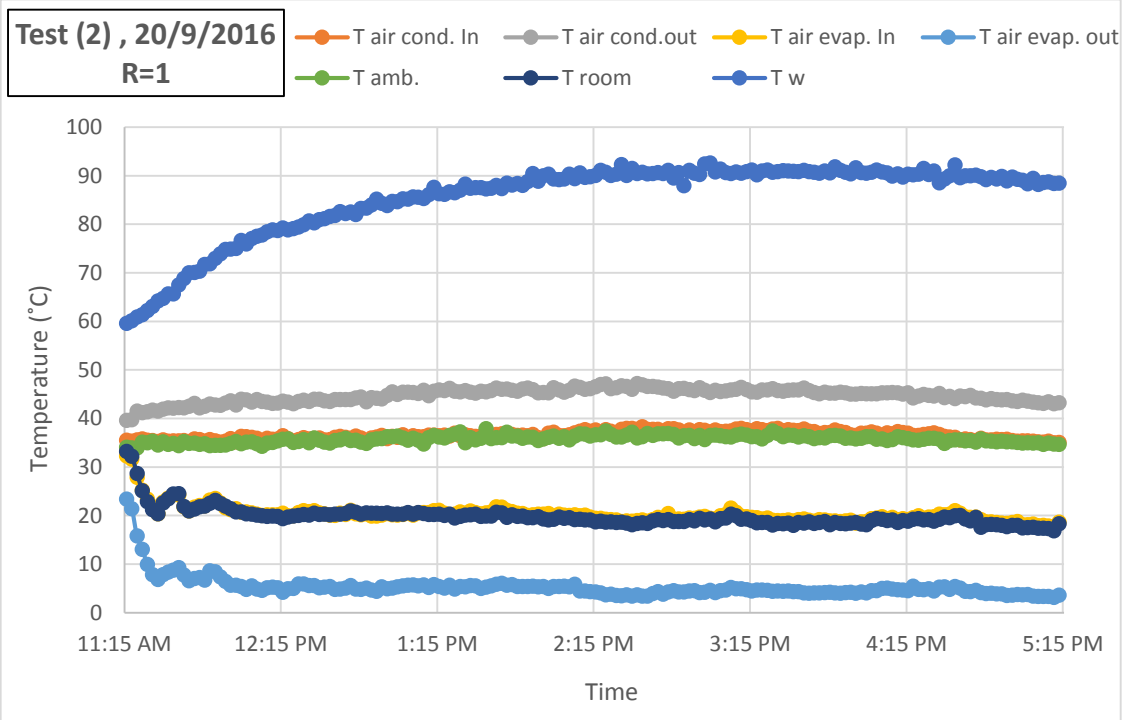

Figure 6b. Air and water temperature with time for test (2).

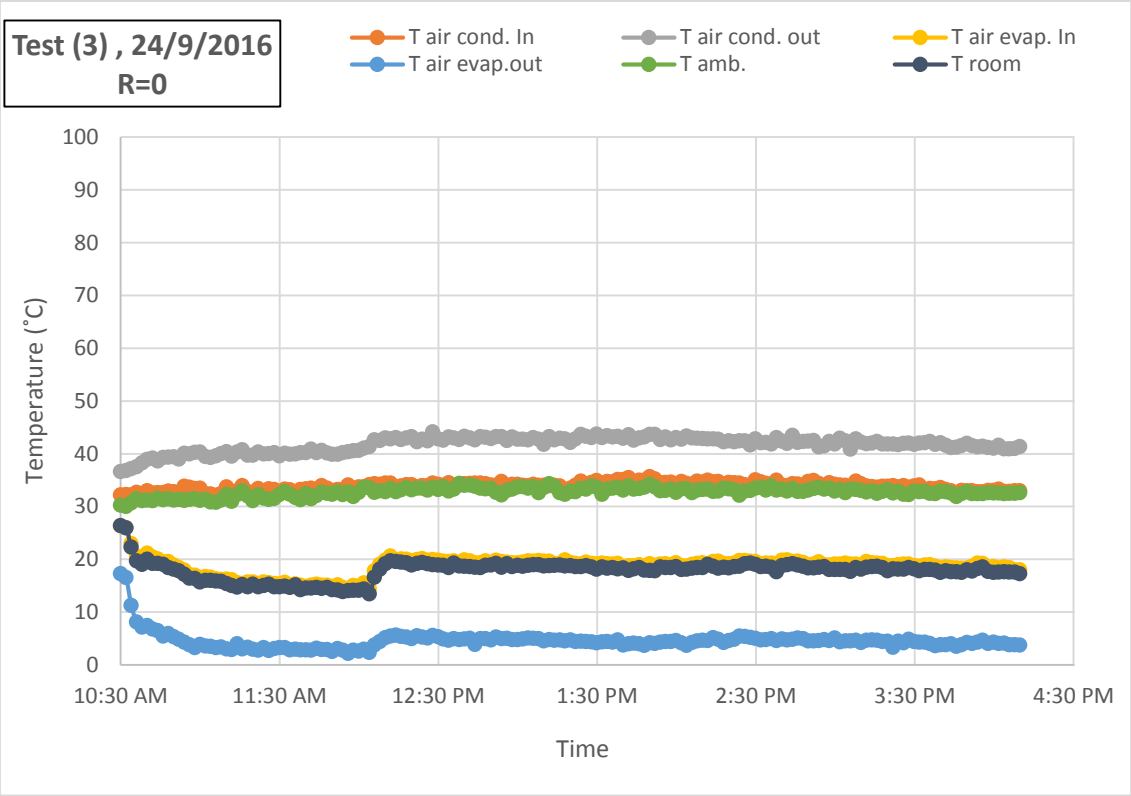

Figure 6c. Air temperature with time for test (3).

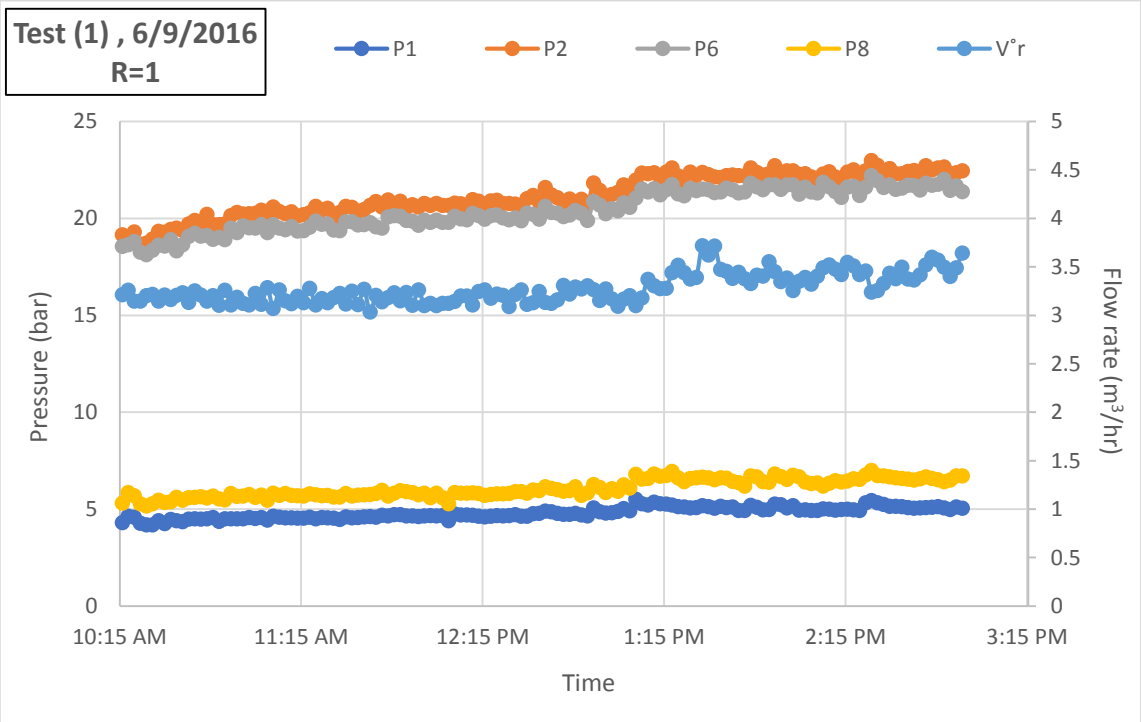

Figure 7a. Refrigerant pressure and volumetric flow rate with time for test (1).

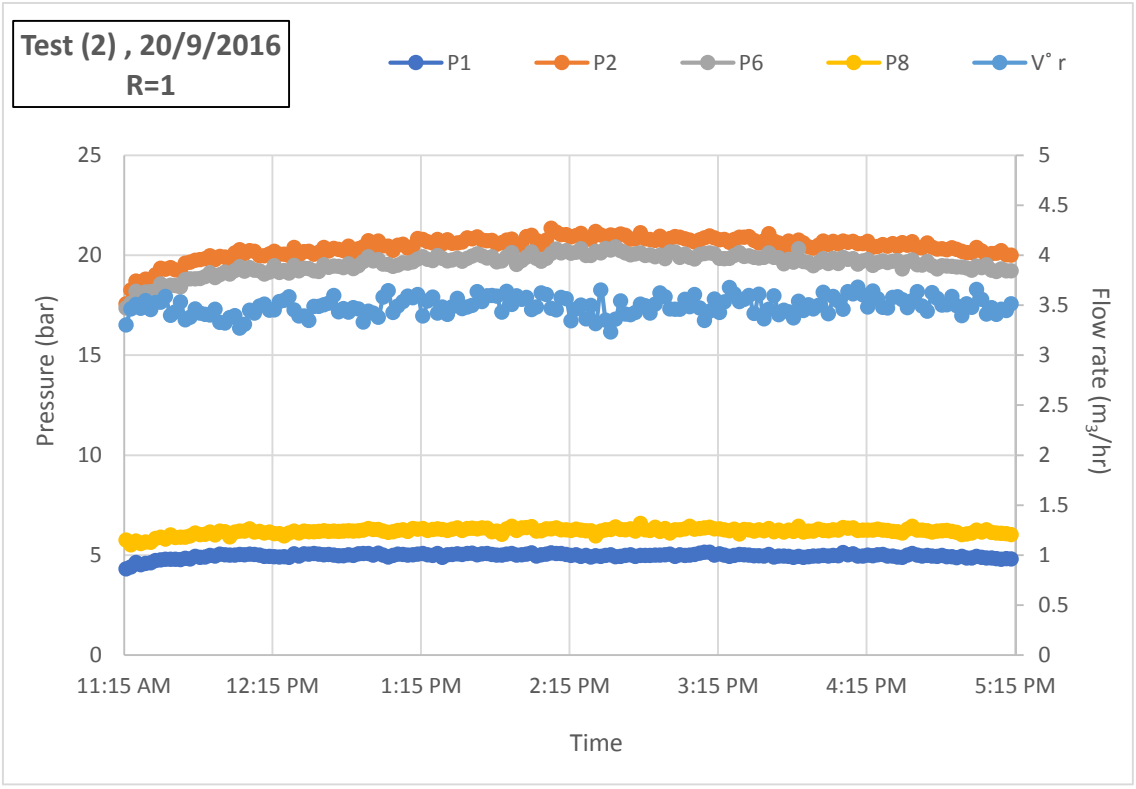

Figure 7b. Refrigerant pressure and volumetric flow rate with time for test (2).

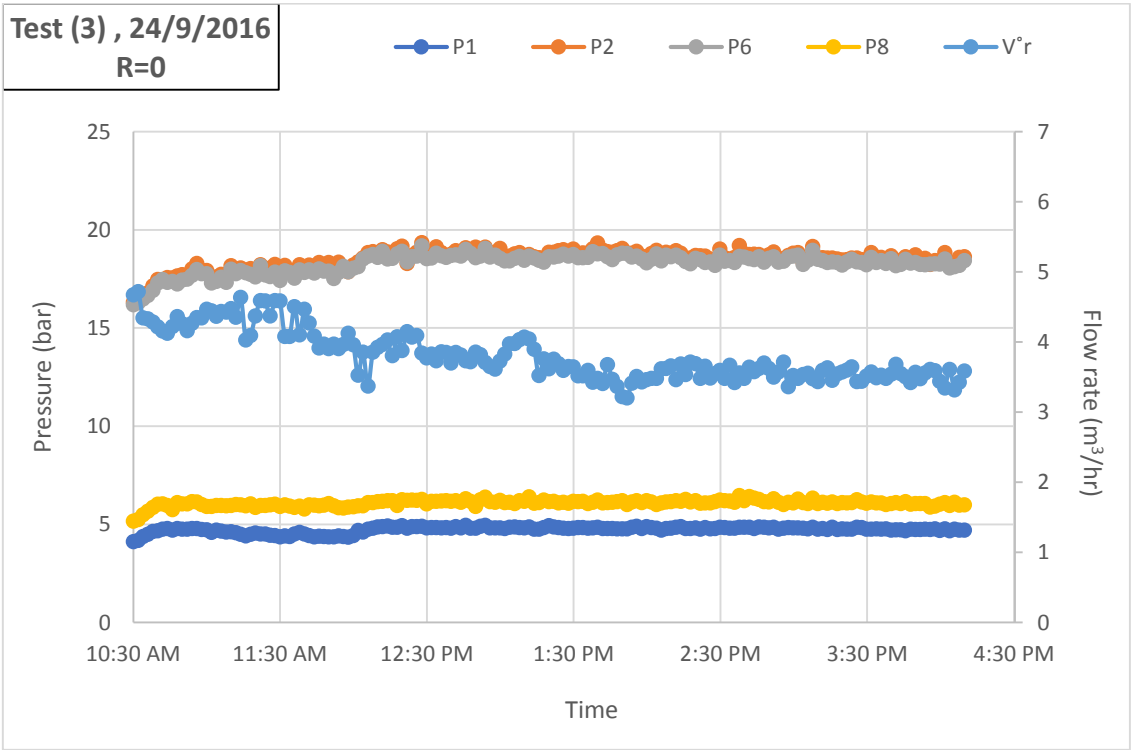

Figure 7c. Refrigerant pressure and volumetric flow rate with time for test (3).

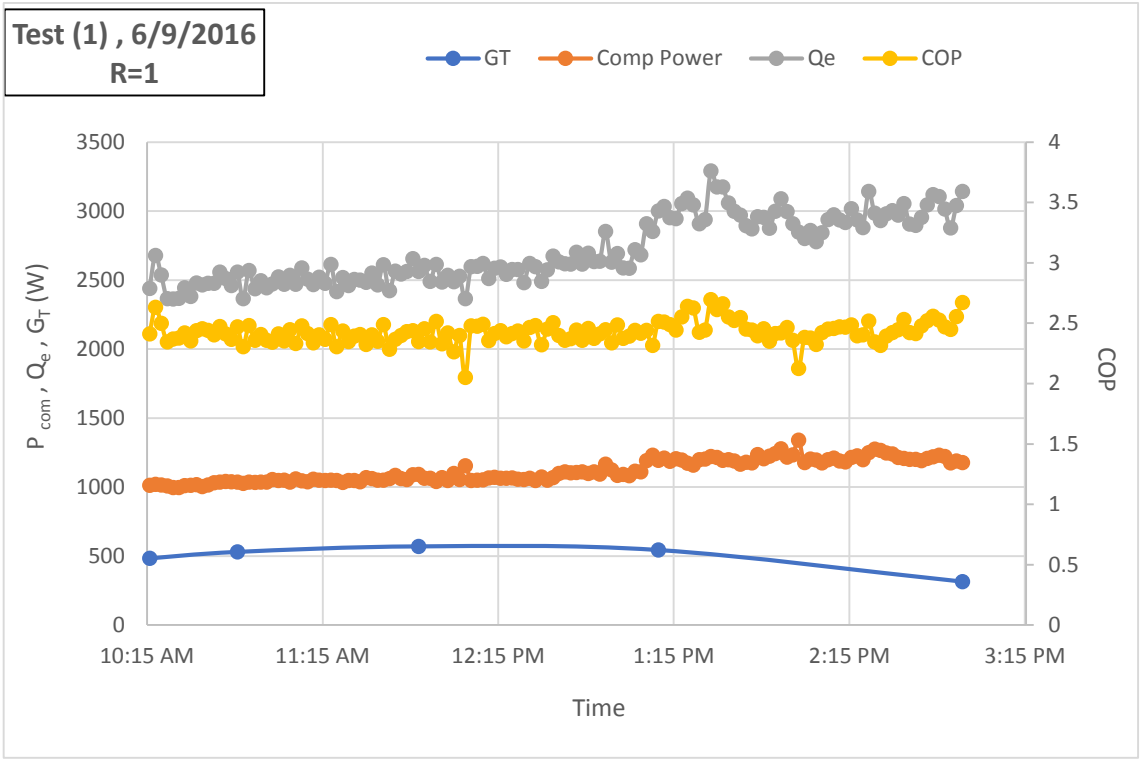

Figure 8a. Power consumption, evaporator heat transfer rate, solar radiation intensityand coefficient of performance with time for test (1).

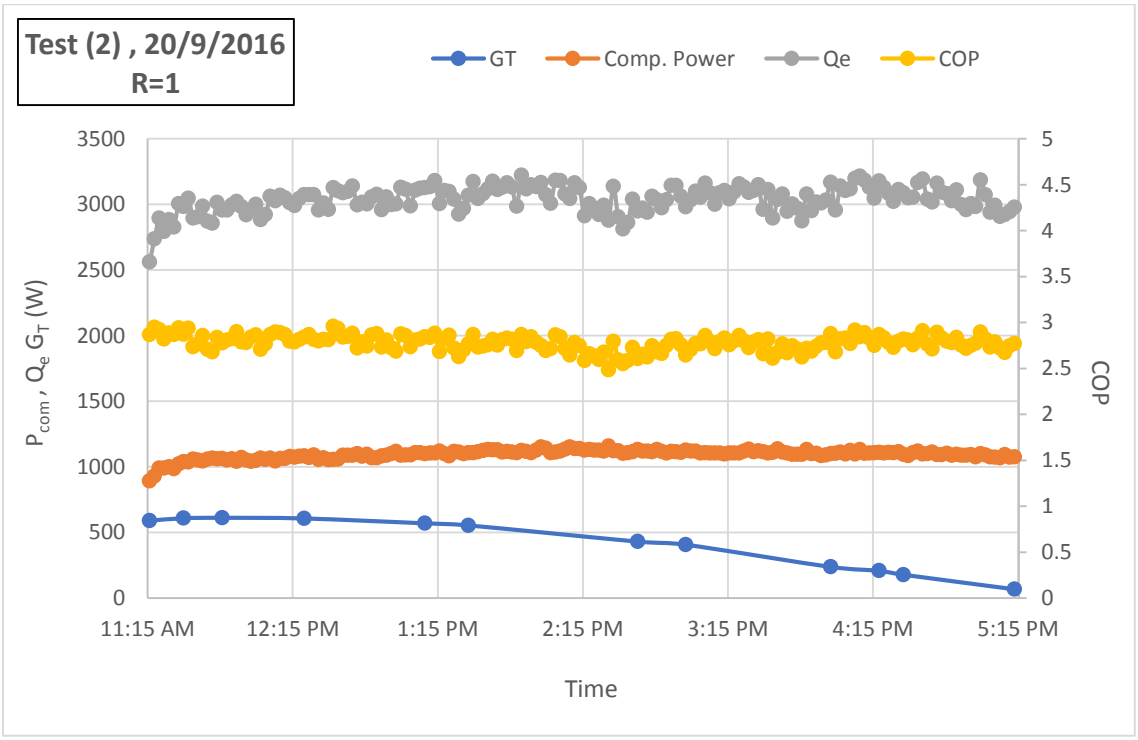

Figure 8b. Power consumption, evaporator heat transfer rate, solar radiationintensity and coefficient of performance with time for test (2).

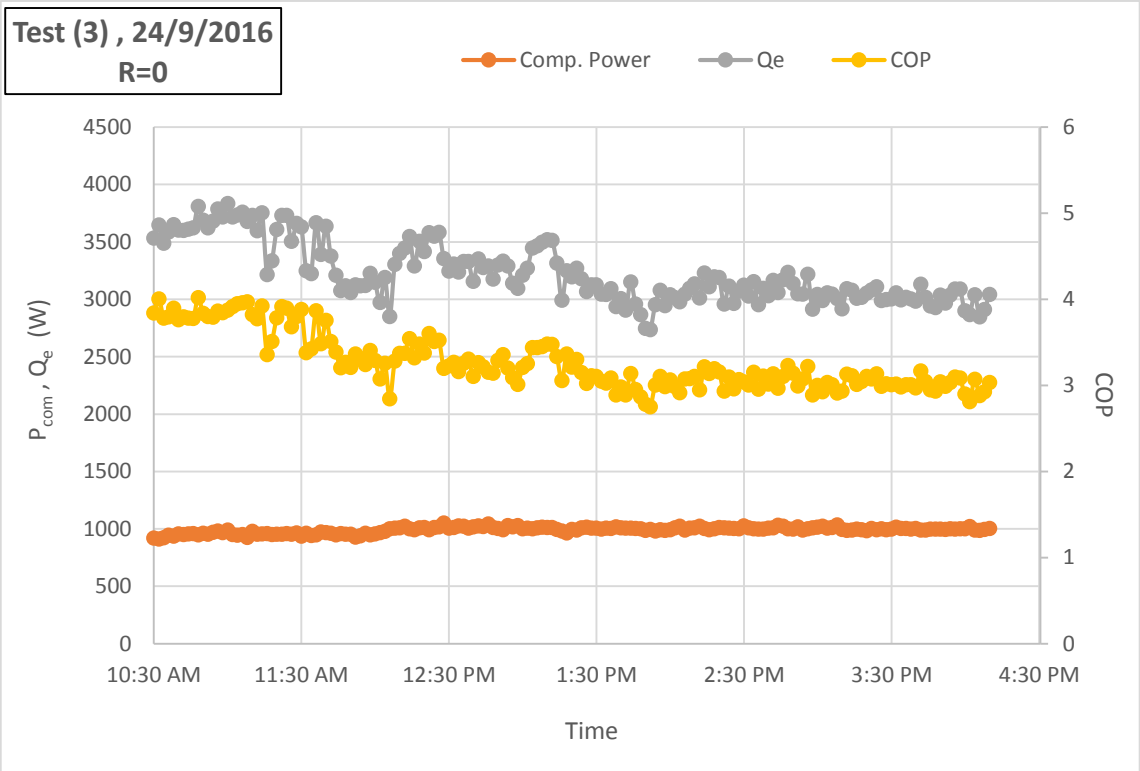

Figure 8c. Power consumption, evaporator heat transfer rateand coefficient of performance with time for test (3).